

Simultaneous Localization and Planning for Cooperative Air Munitions Via Dynamic Programming

Emily A. Doucette¹, Andrew J. Sinclair¹, and David E. Jeffcoat²

¹ Auburn University, Auburn AL 36849, USA

² Air Force Research Laboratory, Eglin Air Force Base FL, USA

Abstract. This work centers on the real-time trajectory planning for the cooperative control of two aerial munitions that are attacking a ground target in a planar setting. Sensor information from each munition is assumed available, and the individual target-location estimates are fused in a weighted least squares solution. The variance of this combined estimate is used to define a cost function. The problem is posed to design munition trajectories that minimize this cost function. This chapter describes the solution of the problem by a dynamic-programming method. The dynamic-programming method establishes a set of grid points for each munition to traverse based on the initial position of the munition relative to the target. The method determines the optimal path along those points to minimize the value of the cost function and consequently decrease the value of uncertainty in the estimate of the target location. The method is validated by comparison to known solutions computed by a variational method for sample solutions. Numerical solutions are presented along with computational run times to indicate that this method proves effective in trajectory design and target location estimation.

1 Introduction

Research is in progress on the cooperative control of air armaments designed to detect, identify, and attack ground targets with minimal operator oversight. One class of this type of armament is wide-area search munitions, which can be deployed in an area of unknown targets. Current development is focused on the possibilities of enhancing munition capabilities through cooperative control. Important work exists in the literature on the two related problems of cooperative search [1,2,3] and the design of optimal trajectories for single observers [4,5,6,7,8,9,10]. The problem of planning optimal trajectories for cooperative observers has been studied using collocation [11,12]. The problem of cooperative attack was previously investigated using variational methods [13]. This chapter presents a method to drastically reduce the computational expense of the previously implemented variational methods by use of the dynamic-programming (DP) method. This problem of designing an attack trajectory that enhances the ability to estimate the target location will be referred to as simultaneous localization and planning (SLAP).

The methods presented in this chapter will be illustrated for a planar problem with two munitions and one stationary target. In the following section, models for the munition motion and sensor performance are presented. Next, the SLAP trajectory design is posed as a DP problem. The cost-sensitivity to grid resolution is then investigated. Finally, the performance of a target-location estimation algorithm is evaluated along the SLAP trajectories and compared to alternative trajectories.

2 Problem Definition

A scenario will be considered with the two-dimensional plane populated by two munitions and a single fixed target. The state of each munition is given by its position in two dimensional space, $\mathbf{x}_1 = [x_1 \ y_1]^\top$ and $\mathbf{x}_2 = [x_2 \ y_2]^\top$. A constant-speed kinematic model is used to describe the motion of the munitions. The heading angles of the munitions are ψ_1 and ψ_2 , and the speed of each munition is v . Here, the heading angles are treated as control variables.

$$\begin{aligned} \dot{x}_1 &= v \cos \psi_1 & ; & & \dot{x}_2 &= v \cos \psi_2 \\ \dot{y}_1 &= v \sin \psi_1 & ; & & \dot{y}_2 &= v \sin \psi_2 \end{aligned} \quad (1)$$

$$\dot{\mathbf{x}}_i = \mathbf{f}_i(\psi_i), \quad i \in \{1, 2\} \quad (2)$$

A variable-speed model could be used; however the additional control variables would increase the complexity of the problem and was not considered here. The two velocities were chosen to be equal for the sake of simplicity. Additionally, each munition is considered to carry a sensor that is capable of measuring the target location in the $x-y$ plane. To design trajectories that improve the estimation of the target location, a model of the sensor measurements and their uncertainties is needed. The target has a position described by $\mathbf{x}_T = [x_T \ y_T]^\top$. The measurement of the target location by each munition, $\tilde{\mathbf{z}}_1 = [\tilde{x}_{T,1} \ \tilde{y}_{T,1}]^\top$ and $\tilde{\mathbf{z}}_2 = [\tilde{x}_{T,2} \ \tilde{y}_{T,2}]^\top$, is modeled as shown in Equation (3).

$$\begin{aligned} \tilde{x}_{T,1} &= x_T + w_{x,1}(0, \sigma_{x,1}) & ; & & \tilde{x}_{T,2} &= x_T + w_{x,2}(0, \sigma_{x,2}) \\ \tilde{y}_{T,1} &= y_T + w_{y,1}(0, \sigma_{y,1}) & ; & & \tilde{y}_{T,2} &= y_T + w_{y,2}(0, \sigma_{y,2}) \end{aligned} \quad (3)$$

The measurement errors from each munition are assumed to be independent of the errors from the other munition. The x and y measurement errors from each individual munition, $w_{x,i}$ and $w_{y,i}$, however, are treated as correlated Gaussian random variables with zero mean and standard deviations of $\sigma_{x,i}$ and $\sigma_{y,i}$, where $i \in \{1, 2\}$. These uncertainties will drive the trajectory design, and they can be selected to model particular sensors.

The error in the target-location measurements from an individual munition is treated as following a zero-mean jointly-Gaussian distribution that is uncorrelated in the down-range and cross-range directions, relative to the true target and munition locations. The errors in these directions, $w_{d,i}(0, \sigma_{d,i})$ and $w_{c,i}(0, \sigma_{c,i})$,

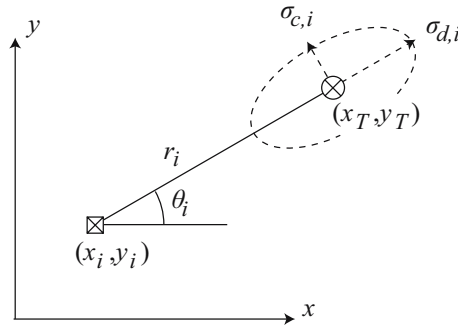


Fig. 1. Measurement of the target by the i th munition and the associated error probability ellipse

can therefore be treated as independent Gaussian random variables. The standard deviations in the down-range and cross-range directions are modeled as functions of the range from the munition to the target.

$$\sigma_{d,i} = 0.1r_i \quad ; \quad \sigma_{c,i} = 0.01r_i \quad (4)$$

These coefficients do not correspond to specifications of any particular sensor, but model a sensor that is more accurate when close to the target and more accurate in the transverse direction than in the radial direction. The uncertainty in the measurement of the target location by the i th munition is illustrated in Figure 1.

From the down-range and cross-range variables, the errors and the covariance matrix in the x and y coordinates can be found.

$$\begin{bmatrix} w_{x,i} \\ w_{y,i} \end{bmatrix} = \begin{bmatrix} \cos \theta_i & \sin \theta_i \\ -\sin \theta_i & \cos \theta_i \end{bmatrix} \begin{bmatrix} w_{d,i} \\ w_{c,i} \end{bmatrix} \quad (5)$$

$$\mathbf{P}_i = \begin{bmatrix} \sigma_{x,i}^2 & \sigma_{xy,i} \\ \sigma_{xy,i} & \sigma_{y,i}^2 \end{bmatrix} = \begin{bmatrix} \cos \theta_i & \sin \theta_i \\ -\sin \theta_i & \cos \theta_i \end{bmatrix} \begin{bmatrix} \sigma_{d,i}^2 & 0 \\ 0 & \sigma_{c,i}^2 \end{bmatrix} \begin{bmatrix} \cos \theta_i & -\sin \theta_i \\ \sin \theta_i & \cos \theta_i \end{bmatrix} \quad (6)$$

Here, θ_i is the bearing angle of the target relative to the i th munition. The range and bearing angle for each target-munition pair are computed as shown below.

$$r_i = \sqrt{(x_T - x_i)^2 + (y_T - y_i)^2} \quad (7)$$

$$\theta_i = \tan^{-1} \left(\frac{y_T - y_i}{x_T - x_i} \right) \quad (8)$$

The measurements provided by both munitions can be fused into a single instantaneous estimate of the target location. This is done using a weighted least-squares estimator (WLSE) [14,15]. The measurements of the target location from

each munition are grouped into a measurement vector $\tilde{\mathbf{z}} = [\tilde{x}_{T,1} \ \tilde{y}_{T,1} \ \tilde{x}_{T,2} \ \tilde{y}_{T,2}]^\top$. This produces a linear measurement model in terms of the target location.

$$\mathbf{z} = \mathbf{H}\mathbf{x}_T + \mathbf{w} \quad (9)$$

$$\mathbf{H} = \begin{bmatrix} 1 & 0 & 1 & 0 \\ 0 & 1 & 0 & 1 \end{bmatrix}^\top; \quad \mathbf{w} = [w_{x,1} \ w_{y,1} \ w_{x,2} \ w_{y,2}]^\top \quad (10)$$

Here, \mathbf{w} is the vector of measurement errors. The covariance of this error vector is given by arranging the covariances from each munition.

$$\mathbf{R} = \begin{bmatrix} \mathbf{P}_1 & \mathbf{0} \\ \mathbf{0} & \mathbf{P}_2 \end{bmatrix} \quad (11)$$

The instantaneous WLSE of the target location and the associated covariance reduce to the following.

$$\mathbf{P} = \begin{bmatrix} \sigma_x^2 & \sigma_{xy} \\ \sigma_{xy} & \sigma_y^2 \end{bmatrix} = (\mathbf{P}_1^{-1} + \mathbf{P}_2^{-1})^{-1} \quad (12)$$

The covariance \mathbf{P} models the uncertainty in the combined target-location estimate based on the positioning of the two munitions relative to the target. The task of designing trajectories for the munitions in order to enhance the estimation performance can now be posed as the following optimal control problem. Consider the state vector $\mathbf{x} = [x_1 \ y_1 \ x_2 \ y_2]^\top$. The heading angles of the munitions can be organized into a control vector $\mathbf{u} = [\psi_1 \ \psi_2]^\top$. The state vector evolves according to the state equation found by grouping Equation (2), $\dot{\mathbf{x}} = \mathbf{f}(\mathbf{u}) = [\mathbf{f}_1^\top \ \mathbf{f}_2^\top]^\top$. For boundary conditions, the initial positions of the munitions will be considered a given, and the final position of munition 1 is required to be the target location, $x_1(t_F) = x_T$ and $y_1(t_F) = y_T$. The final position of munition 2 is free.

The goal will be to find the trajectories that minimize the following cost function, which is based on the WLSE covariance.

$$J = \int_0^{t_F} (\sigma_x^2 + \sigma_y^2) dt \quad (13)$$

The variances of each target location are functions of the states describing the munition configuration. Clearly, this cost function emphasizes the uncertainty over the entire trajectory. Alternative cost functions could be defined using other metrics of the covariance matrix, but these were not investigated here.

3 Dynamic-Programming Approach

The above nonconvex problem has previously been solved using a variational method [13]. Although these solutions demonstrated that significant improvements in the target-location estimate could be achieved, the method was too

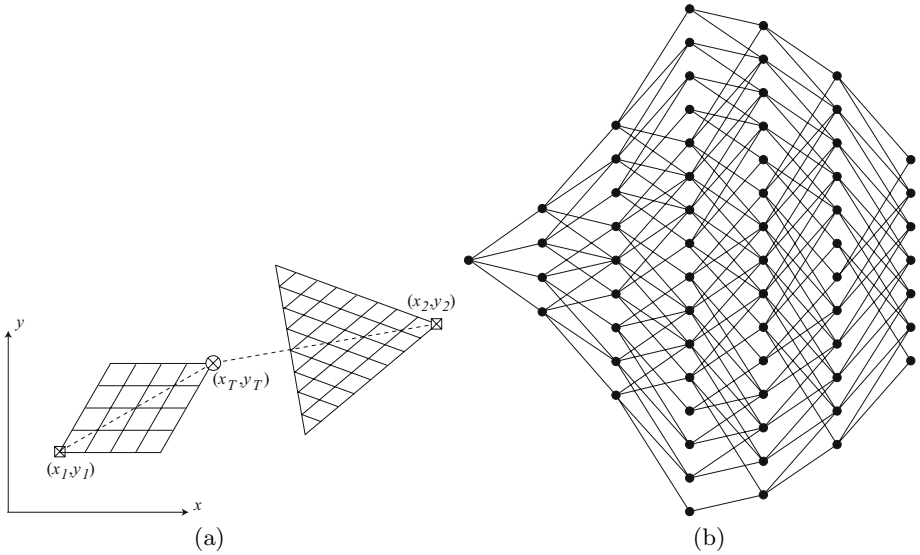


Fig. 2. Example of (a) path grids and (b) DAG where $n = 64$ and $m = 168$ and all edges are directed from left to right

computationally expensive for implementation. This section describes a solution of the problem by dynamic programming (DP), with the goal of reducing computational expense.

Whereas variational methods consider a continuous range of heading angles at any instant in time, the approach considered here only allows a discrete number of possible headings at discrete instants in time. Admissible trajectories were selected considering Equation (2). The trajectories were limited to two possible heading angles at each decision instant. In between decision points, the trajectories follow constant headings. This discretization generates a grid of possible trajectories, as illustrated in Figure 2 (a). This grid of physical points through which the munitions may travel is referred to as the path grid. It is noteworthy that the candidate paths are based on the simple vehicle model in Equation (2); however, the path planning generated from this model could be applied to a higher-order system.

The path grids were laid out for each munition and were structured such that they were symmetric about a reference line from the initial state to the target location. The expansion of this grid is variable about the reference line by an angle, α . Because the results of the variational method showed that the munitions tended to approach the target at orthogonal headings, the path grid was of variable width to allow for outward sweeps. The degree of expansion was determined based on the initial positions of the munitions relative to the target.

The nodes were organized into subsets of nodes that could be reached in a given amount of time. Consequently, the time increment between layers was also assumed constant between each layer. This time increment is calculated from

the initial range of the munition that will strike the target, which is assumed to always be the closer of the two munitions. The same time step is used for both munitions in order to preserve synchronized motion of the munitions.

This algorithm implements the Bellman-Ford model for trajectory optimization through dynamic programming in Fortran 77 [16]. Once a cost function is defined and a cost corresponding to each possible set of paths for each munition is calculated according to Equation (13), the combinatorial possibilities of physical node locations for the two munitions were used to form the vertices of a directed acyclic graph (DAG) with n vertices and m edges. Each vertex represents a particular location for each munition at a particular instant in time, and each edge corresponds to the cost value associated with the munitions traveling to those particular locations. The graph is directed and acyclic because the paths must follow the flow of time.

The vertices are arranged into subsets, where each subset represents a particular instant in time. Once the cost along each edge of the DAG is computed, the algorithm marches backward in time from the last layer of vertices to the first vertex to determine the lowest possible cost and the path that produces it. At each subset, the optimal path is computed by comparing the costs to proceed forward. That path and cost are then stored and the algorithm works backwards to the preceding subset, continuing this process until it reaches the initial vertex. The DAG associated with the path grid in Figure 2 (a) is shown in Figure 2 (b). Solutions for this type of graph can be computed in $\mathcal{O}(m)$ time.

Example trajectories produced by the DP method are shown in Figures 3 and 4 using $n = 64$ and $m = 168$. The DP trajectories are also compared to trajectories computed from the variational method. A third order curve fit was used to obtain the smooth trajectories from the grid points of the path grids. The trends of the DP trajectories capture those of the variational method. This is also evidenced by a minor increase in the final cost of approximately 7.75% in each problem, as shown in Table 1. When paired with a computational run-time of 0.1 sec on a 2GHz PC for the DP method, and the advantage of deterministic

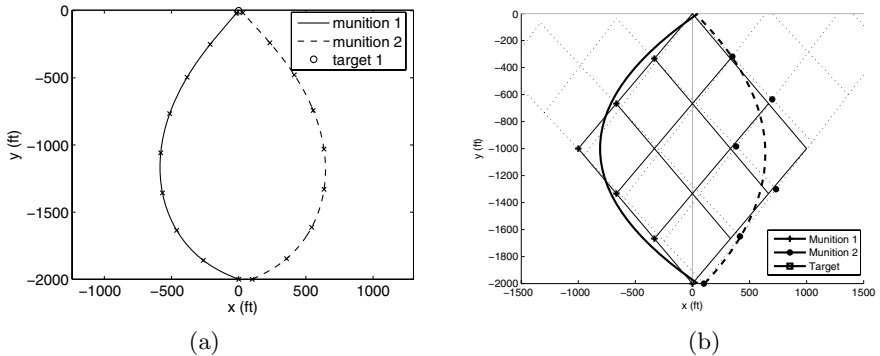


Fig. 3. Problem 1 SLAP trajectories from variational (a) and DP (b) methods

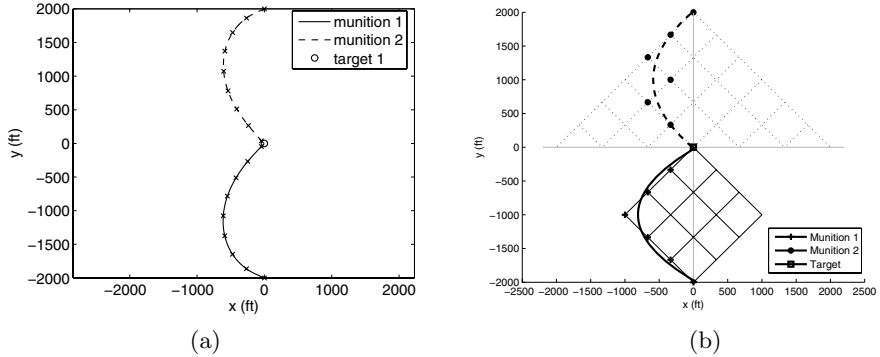


Fig. 4. Problem 2 SLAP trajectories from variational (a) and DP (b) methods

Table 1. Cost for sample SLAP trajectories

Problem	DP Method Cost $n = 64$	DP Method Cost $n = 27$	Variational Method Cost
1	$1.7181 * 10^4$	$1.7209 * 10^4$	$1.59 * 10^4$
2	$2.0317 * 10^4$	$2.0318 * 10^4$	$1.89 * 10^4$

run time, these cost values confirm the effectiveness of this method to the SLAP problem.

4 Cost Sensitivity to Grid Resolution

In implementing the DP method, the resolution of the path grids and the resulting DAG must be selected. In order to determine an appropriate resolution, the sensitivity of the cost to grid resolution was investigated. A lower resolution DAG with $n = 27$ and $m = 70$ was created. The resulting increase in performance cost was less than 1%, as shown in Table 1. This low sensitivity to grid resolution did not motivate the investigation of resolutions greater than $n = 64$.

5 Estimation Performance

The impact of the trajectories on the target-location estimation can now be evaluated. Although the trajectories were designed using a cost function based on the variances from a continuous WLSE algorithm, the estimation performance will be evaluated using a recursive weighted least squares estimation (RWLSE) algorithm with discrete measurement updates. The estimates computed using the DP trajectories are compared to estimates using the variational method and following trajectories from the initial conditions straight to the target location (STT trajectory). In each case, noisy measurements were simulated using the

measurement model in Equation (4). The measurements were generated by use of the RANDN command in MATLAB to generate a normal distribution of random numbers.

The munition sensors were assumed to collect measurements of the target location at a rate of 10 Hz. The RWLSE algorithm operated as follows to determine the estimate and the uncertainty at the k th time step [14,15]. The current estimate is computed as follows.

$$\mathbf{K}_k = \mathbf{P}_{k-1} \mathbf{H}^\top (\mathbf{H} \mathbf{P}_{k-1} \mathbf{H}^\top + \mathbf{R})^{-1} \quad (14)$$

$$\hat{\mathbf{x}}_k^{(T)} = \hat{\mathbf{x}}_{k-1}^{(T)} + \mathbf{K}_k (\mathbf{z}_k - \mathbf{H} \hat{\mathbf{x}}_{k-1}^{(T)}) \quad (15)$$

The current covariance matrix is computed as shown.

$$\mathbf{P}_k = \begin{bmatrix} \sigma_{x,k}^2 & \sigma_{xy,k} \\ \sigma_{xy,k} & \sigma_{y,k}^2 \end{bmatrix} = (\mathbf{P}_{k-1}^{-1} + \mathbf{H}_k^\top \mathbf{R}_k^{-1} \mathbf{H}_k)^{-1} \quad (16)$$

To compare the estimation performance along the different trajectories, the size of the one-sigma uncertainty ellipsoid in the target-location estimate can be used as a metric. At the k th time step, this is given by the product of π with the square root of the product of the eigenvalues of \mathbf{P}_k . In particular, the ellipsoid size at two seconds prior to impact ($(t_F - 2)$ seconds) will be highlighted. Although t_F is different for each trajectory, at this point in time munition 1 is roughly 600 ft from the target.

Using the initial condition of $x_1(0) = 0$ ft, $y_1(0) = -2000$ ft, $x_2(0) = 100$ ft, and $y_2(0) = -2000$ ft, two munitions on STT trajectories correspond to a one-sigma uncertainty ellipse with an area of 39.7 ft^2 at $(t_F - 2)$ sec, with $t_F = 6.67$, sec. When the two munitions follow the SLAP trajectories obtained through the variational and DP methods shown in Figure 3 however, the area is reduced as shown in Table 2. The error histories for a sample simulation with noisy measurements and three-sigma error bounds ($\pm 3\sigma_{x,k}$ and $\pm 3\sigma_{y,k}$) generated by the RWLSE algorithm are shown in Figure 5. Figure 5(a) shows the errors in the x and y estimates of the target location using the variational method trajectories. Figure 5(b) show the errors using the DP trajectories. Both trajectories give similar, relatively good performance in estimating the target location, however the DP trajectory has slightly slower convergence. This highlights the difference between the uncertainty ellipse area as a performance metric and the cost function used in generating the paths.

Table 2. Area of one-sigma uncertainty ellipse

Problem	STT	Variational Method	DP Method
1	39.7 ft^2	9.1 ft^2	24.5 ft^2
2	40.8 ft^2	9.3 ft^2	23.5 ft^2

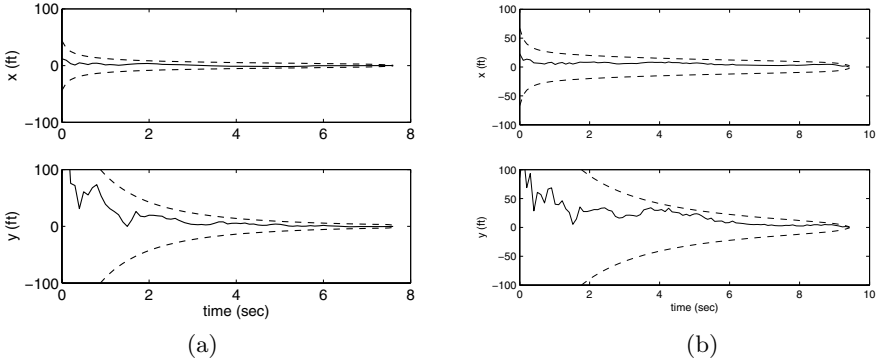


Fig. 5. Estimation errors using (a) Variational Method and (b) DP trajectories with $x_2(0) = 100$ ft, and $y_2(0) = -2000$ ft

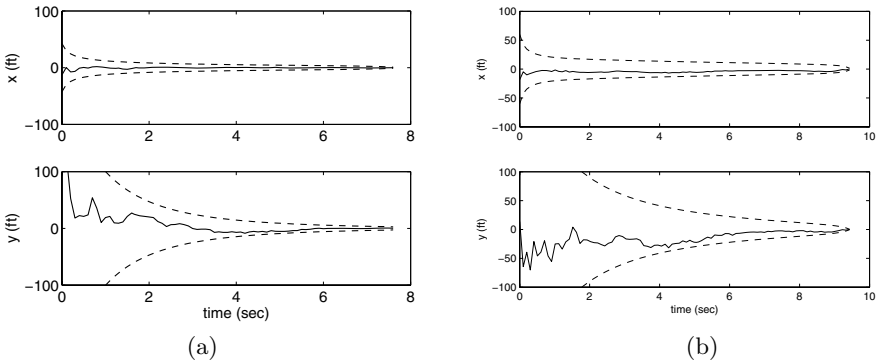


Fig. 6. Estimation errors using (a) Variational Method and (b) DP trajectories with $x_2(0) = 0$ ft, and $y_2(0) = 2000$ ft

Moving munition 2 to the initial condition $x_2(0) = 0$ ft, and $y_2(0) = 2000$ ft corresponds to an uncertainty ellipse with an area of 9.3 ft^2 for the variational method trajectories. With a mesh expansion angle of $\pi/4$, the resulting uncertainty ellipse area was 23.5 ft^2 for the DP trajectories. For these initial conditions, the error histories for a sample simulation with noisy measurements and three-sigma error bounds generated by the RWLSE algorithm are shown in Figure 6.

6 Conclusions

Careful trajectory design can have a significant impact on target-location estimation. In this work, the DP approach was used to demonstrate that SLAP trajectories are practical for real-time implementation. The advantage of this approach is that discretization in both time and spatial coordinates results in a DAG on which the corresponding problem can be solved in a deterministic

amount of computation. This allows grid resolution to be selected based on the available computational resources and desired performance.

More accurate target-location estimation could allow more accurate strike capability or the ability to attack the targets that are difficult to detect. Further work is needed to demonstrate the impact of these estimation enhancements on guidance and control performance. In future implementations, heuristic methods may be developed based on insight gained from solutions of the optimal control problem. Additionally, an algorithm could be developed to allow for an adaptive mesh expansion angle. The DP approach will still be a useful development tool to cheaply investigate various solutions.

Acknowledgment

The authors are grateful to Clayton W. Commander, Air Force Research Lab, for his helpful discussion of shortest-path algorithms.

References

1. Chandler, P.R., Pachter, M., Nygard, K.E., Swaroop, D.: Cooperative control for target classification. In: Murphey, R., Pardalos, P.M. (eds.) *Cooperative Control and Optimization*, pp. 1–19. Kluwer, Netherlands (2002)
2. Jeffcoat, D.E.: Coupled detection rates: An introduction. In: Grundel, D., Murphey, R., Pardalos, P.M. (eds.) *Theory and Algorithms for Cooperative Systems*, pp. 157–167. World Scientific, New Jersey (2004)
3. Frew, E., Lawrence, D.: Cooperative stand-off tracking of moving targets by a team of autonomous aircraft. In: AIAA-2005-6363. AIAA Guidance, Navigation, and Control Conference, San Francisco, California (August 2005)
4. Fawcett, J.A.: Effect of course maneuvers on bearings-only range estimation. *IEEE Transactions on Acoustics, Speech, and Signal Processing* 36(8), 1193–1199 (1988)
5. Hammel, S.E., Liu, P.T., Hilliard, E.J., Gong, K.F.: Optimal observer motion for localization with bearing measurements. *Computers and Mathematics with Applications* 18(1-3), 171–180 (1989)
6. Logothetis, A., Isaksson, A., Evans, R.J.: Comparison of suboptimal strategies for optimal own-ship maneuvers in bearings-only tracking. In: *American Control Conference*, Philadelphia, Pennsylvania (June 1998)
7. Passerieux, J.M., Van Cappel, D.: Optimal observer maneuver for bearings-only tracking. *IEEE Transactions on Aerospace and Electronic Systems* 34(3), 777–788 (1998)
8. Oshman, Y., Davidson, P.: Optimization of observer trajectories for bearings-only target localization. *IEEE Transactions on Aerospace and Electronic Systems* 35(3), 892–902 (1999)
9. Frew, E.W., Rock, S.M.: Trajectory generation for constant velocity target motion estimation using monocular vision. In: *IEEE International Conference on Robotics & Automation*, Taipei, Taiwan (September 2003)
10. Watanabe, Y., Johnson, E.N., Calise, A.J.: Vision-based guidance design from sensor trajectory optimization. In: AIAA-2006-6607. AIAA Guidance, Navigation, and Control Conference, Keystone, Colorado (August 2006)

11. Grocholsky, B.: Information-Theoretic Control of Multiple Sensor Platforms. Ph.D thesis, University of Sydney, Sydney, Australia (2002)
12. Ousingsawat, J., Campbell, M.E.: Optimal cooperative reconnaissance using multiple vehicles. *Journal of Guidance, Control, and Dynamics* 30(1), 122–132 (2007)
13. Sinclair, A.J., Prazencia, R.J., Jeffcoat, D.E.: Simultaneous localization and planning for cooperative air munitions. In: Hirsch, M.J., Pardalos, P.M., Murphey, R., Grundel, D. (eds.) *Advances in Cooperative Control and Optimization*. LNCIS, vol. 369, pp. 81–94. Springer, Heidelberg
14. Stengel, R.F.: *Optimal Control and Estimation*. Dover, New York (1986)
15. Crassidis, J.L., Junkins, J.L.: *Optimal Estimation of Dynamic Systems*. Chapman & Hall/CRC, Boca Raton (2004)
16. Bellman, R.E., Dreyfus, S.E.: *Applied Dynamic Programming*. Princeton University Press, Princeton (1962)